Integral apolipoproteins increase surface-located triacylglycerol in intact native apoB-100-containing lipoproteins

Elizabeth Boyle-Roden[1,*] and Rosemary L. Walzem[†]

Department of Nutrition and Food Science,* University of Maryland, College Park, MD 20742; and Department of Poultry Science,† Texas A&M University, College Station, TX 77843-2472

Abstract **High-resolution NMR was used to measure the presence and quantity of triacylglycerol (TAG) in the surface of intact native apolipoprotein B-100-containing lipoprotein particles that are made by chickens in response to estrogen treatment and that in hens are deposited in yolk follicles (VLDLy). Integration of ^{13}C NMR resonances shows that intact VLDLy particles contain more surface TAG (5.1 ± 0.6 mol%, 6.7 ± 0.8 weight %) than predicted by apolipoprotein-free models using similarly acyl-heterogenous TAG. Change in downfield chemical shift values of surface to core TAG in VLDLy was 0.8 ppm compared with 1.3 ppm in vesicles prepared with purified egg phosphatidylcholine and TAG isolated from the VLDLy, indicating that reduced surface TAG hydration may contribute to the resistance to lipase hydrolysis characteristic of this lipoprotein species. Apolipoprotein-mediated changes in surface lipid composition and lipid hydration provide possible general mechanisms for selectivity in lipoprotein substrate characteristics.**—Boyle-Roden, E., and R. L. Walzem. **Integral apolipoproteins increase surface-located triacylglycerol in intact native apoB-100-containing lipoproteins.** ***J. Lipid Res.*** **2005.** 46: **1624–1632.**

Supplementary key words apolipoprotein B-100 • yolk-deposited very low density lipoproteins • ^{13}C nuclear magnetic resonance • surface lipid • estrogen • birds

Lipoprotein particle metabolism exemplifies the complex biological chemistry that is reliant on the integrated function of apolipoproteins, enzymes, and transfer proteins and fundamentally dependent on the accessibility of lipoprotein lipids to those proteins. Mechanistic studies often focus on protein-based interactions that regulate particle metabolism and uptake. Tremendous advances in genetic manipulation and protein chemistry continue to drive rapid progress in these areas. Studies with model triacylglycerol (TAG)-rich lipoprotein particles show that metabolism also depends on surface lipid composition (1, 2). Paradoxical outcomes, such as increased apparent lipase activity with low-affinity substrates, occur when only whole particle lipid substrate composition is considered (2). This occurs presumably because most reactions involving nonpolar lipids take place at the interface between the particle and the surrounding aqueous medium; thus, both the affinity of the enzyme for the interface and the specific accessibility of the substrate molecules to the lipase drive reaction kinetics, rather than total particle lipid content per se (2). The presence of relatively small quantities of both substrate and nonsubstrate lipids can alter the affinity of an enzyme for the interface (3–5). Thus, the more metabolically relevant description of lipoprotein particle lipids is their specific composition and concentration within the surface layer.

Lipoprotein particles possess an outer amphipathic layer of proteins, unesterified cholesterol (UC), and phospholipids (PLs) and an inner core of nonpolar TAG and cholesteryl ester (CE). The major surface components of apolipoprotein B-100 (apoB-100)-containing lipoprotein particles are well characterized in terms of their general mass, orientation, and surface area (6–9). Miller and Small (8) prepared emulsions from the lipids extracted from human VLDLs and then broke these same emulsions by ultracentrifugation to obtain a pelleted surface and a floating core, or oil, phase. Lipids present in each physically separated phase were quantitated and used to determine the distribution of lipid classes between surface and core components of these emulsions. TAG accounted for 3.63 ± 0.6 weight percent (wt%) of the surface of those emulsions, whereas in a similarly prepared sample of mon-

Manuscript received 30 October 2004 and in revised form 21 March 2005 and in re-revised form 6 May 2005.

Published, JLR Papers in Press, June 1, 2005.
DOI 10.1194/jlr.M400434-JLR200

Abbreviations: apoB-100, apolipoprotein B-100; CE, cholesteryl ester; DES, diethylstilbestrol; NOE, nuclear Overhauser enhancement; PC, phosphatidylcholine; PL, phospholipid; TAG, triacylglycerol; UC, unesterified cholesterol; VLDLy, yolk-deposited very low density lipoprotein.

[1] To whom correspondence should be addressed.
e-mail: eboyle-r@chemistry.ohio-state.edu

key lymph chylomicrons, TAG was determined to constitute 2.1 wt% of the surface phase. The chemical composition data from these experiments were combined with hydration data to create four components, namely neutral (TAG + CE), polar [phosphatidylcholine (PC) + phosphatidylethanolamine + sphingomyelin + lysophosphatidylcholine], UC, and water; subsequently, they were used to construct ternary phase diagrams. To model relationships found in biological systems, the authors made detailed analyses within the 90% water region of the diagram. Specifically, they predicted the distribution of UC between the surface and core phases of intact lipoprotein particles as well as particle diameters. They concluded that the methods worked well, that the potential effect of apolipoprotein on the distribution of UC could be assessed using the phase diagrams, and that the presence of apolipoproteins in intact lipoprotein particles did not significantly alter UC partitioning. However, they also concluded that the effect of apolipoproteins on the partitioning of neutral lipids such as TAG and CE could not be determined (8).

Successful assembly of VLDL requires the cotranslational association of apoB-100 with polar and neutral lipids within the rough endoplasmic reticulum (10, 11). The essentiality of this association between lipids and apolipoprotein suggests that specific lipid and apolipoprotein interactions are necessary for proper particle formation (6). Moreover, apolipoproteins are essential for normal lipoprotein particle metabolism.

Ryan's group (12) used ^{13}C NMR to document the presence of surface-located diacylglycerol in insect lipoproteins. Miller and Small (8) did not find diacylglycerol in VLDL preparations, but they did find this lipid wholly partitioned into the surface fraction of coalesced monkey lymph chylomicron preparations. Insect lipoproteins do not contain TAG, the major metabolic energy storage molecule of avians and mammals (12). However, TAG has also been documented in PL surfaces of vesicles and emulsions by the measurement of ^{13}C carbonyl-enriched TAG (13–18). Measurements of the amount of TAG in the surface of PL vesicles generally agree with the emulsion data (8, 9), but neither system contains protein. The identification of TAG in the surface of PL-stabilized emulsions indicates that TAG is likely present in the surface of native lipoproteins but is of insufficient ^{13}C signal intensity to be detected by NMR (17). Thus, although numerous ^{13}C NMR spectra of native lipoproteins have been published, surface-located TAG has not previously been detected (19–22) by this approach.

We increased the ^{13}C signal intensity of TAG by taking advantage of the estrogen-dependent augmentation of hepatic VLDL assembly processes that underlie yolk formation in birds (23). Hens secrete large numbers of VLDLs with highly uniform physical dimensions and chemical composition known as VLDLy because they are targeted for yolk deposition (24). VLDLy are TAG-rich (>60% particle lipid) and relatively CE-poor (<5% particle lipid) particles surrounded by a surface composed of integrally associated apoB-100, PL, and UC (25). VLDLy are half the diameter of non-yolk-targeted VLDL, 25–30 nm in diameter compared with 50–60 nm (24). Each VLDLy particle from *Gallus domesticus* contains one apoB-100 molecule in combination with 16–23 dimers of an estrogen-induced apoVLDL$_{II}$ (25, 26). ApoVLDL$_{II}$ is thought to mediate particle diameter reduction (25) and functions to inhibit LPL activity (27, 28). Thus, VLDLy are poorly metabolized in the vascular space and, as a result, are ideally suited to transport TAG to the developing egg yolk follicles (24). Exogenous estrogen administration rapidly increases VLDLy assembly even in fasting male birds (29). In the absence of active ovarian follicular uptake, VLDLy accumulates to high concentrations in the blood vasculature and is readily harvested from plasma (30). Thus, birds fed [1-^{13}C]palmitate and tri-[1-^{13}C]oleoylglycerol could incorporate isotopically enriched lipid into native VLDLy to enhance NMR signal and reveal surface-located TAG. The objective of this study was to produce native lipoprotein particles enriched in carbonyl ^{13}C-labeled TAG for investigations of surface lipid composition.

MATERIALS AND METHODS

[1-^{13}C]palmitate and tri-[1-^{13}C]oleoylglycerol were purchased from Cambridge Isotope Laboratories (Cambridge, MA). Pentadecanoic acid, heptadecanoic acid, and fatty acid methyl ester standards were purchased from Nuchek Prep, Inc. (Elysian, MN); olive oil (Star Extra Light) was purchased from a local grocery store (Safeway, Davis, CA). Myverol 18-99 (distilled monoglycerides) was from Eastman Chemical Co. (Kingsport, TN). Deuterium oxide (99.9%) was purchased from Aldrich Chemical Co. (Milwaukee, WI). Thin-layer chromatography plates (K6 silica gel 60 Å) were purchased from Whatman, Inc. (Clifton, NJ). Protein assay reagents, sodium cholate, oleic acid, diethylstilbestrol (DES), and GPO-Trinder enzymatic TAG test kits were purchased from Sigma Chemical Co. (St. Louis, MO). Day-old Hy-Line W36 male chicks were purchased from Hy-Line International (Lakeview, CA), fed a commercial starter diet (Start 'n Grow, 3% fat; Purina Mills, St. Louis, MO), and provided 12 h of light per day. The basal diet was supplemented with 60 g/kg corn oil for at least 10 days before study. Animal care committees of both institutions approved the bird husbandry and experimental protocols.

Preparation of intubation emulsions

Emulsion mixtures were freshly prepared on the day of use by slowly dispersing pentadecanoic acid, palmitic acid, and/or trioleoylglycerol in olive oil with stirring, followed by the addition of distilled monoglycerides. Sodium cholate solution was then added, and the resulting emulsion was mixed for 1 h at 45°C. The compositions of intubation mixtures used in the three studies are shown in **Table 1**. Treatment birds were intubated with warm emulsions containing [1-^{13}C]palmitate and tri-[1-^{13}C]oleoylglycerol, and their matched controls were intubated with emulsions composed of the same amounts of native (non-^{13}C-enriched) palmitate and trioleoylglycerol.

Intubation and production of VLDLy

Cockerels of the Hy-Line W36 strain, 0.4–2.0 kg body weight, were used in these studies. The time required to reduce mean circulating VLDL particle diameter to that typical for VLDLy was established by injecting six cockerels with a 6 mg/kg dose of the synthetic estrogen DES dissolved in olive oil into the inguinal skin

TABLE 1. Composition of intubation mixtures

Emulsion Component	Study 1: Native Lipid	Study 2: [1-^{13}C]palmitate	Study 3: tri-[1-^{13}C]oleoylglycerol and [1-^{13}C]palmitate
		g	
Olive oil	10.0	3.9	2.0
Palmitic acid	3.9	2.0	1.0
Triolein	—	—	2.0
Pentadecanoic acid	0.1	0.1	0.2
Myverol 18-99	0.8	0.4	0.4
Sodium cholate	0.1	0.05	0.05
Water	20.0	10.0	10.0

Intubation mixtures were prepared the day of use by slowly melting and dispersing free fatty acid into oil with stirring, followed by the addition of Myverol 18-99. Sodium cholate in water was then added, and the resulting emulsion was mixed for 1 h at 45°C. Birds were orally intubated with 10 ml of the specified lipid emulsion followed by an additional intubation of 25 ml of 0.04 M sodium cholate in water. Treatment birds were intubated with [1-^{13}C]palmitate and tri-[1-^{13}C]oleoylglycerol, and control birds were intubated with natural palmitate and triolein.

fold. Blood was drawn before and again at 4, 7, and 20 h after DES injection for VLDL isolation from plasma. To study fatty acid incorporation into VLDLy, feed was removed from four birds on the evening before intubation. Two birds were injected with DES, and two served as vehicle-injected controls. The next day, 20 gauge, 1.25 inch catheters (Insyte; Becton Dickinson, Sandy, UT) were inserted into the humeral vein, capped (Argyle intermittent infusion plugs; Sherwood Medical, St. Louis, MO), and flushed with 2 ml of sterile saline. Blood clotting in the catheter was prevented by filling the end cap with 0.5 ml of sterile saline containing 2.65 mM Na_4-EDTA. Birds were intubated first with 10 ml of a lipid emulsion that contained pentadecanoic acid as a tracer fatty acid (Table 1, study 1), followed by 25 ml of 0.04 M sodium cholate in water at 18 h after DES treatment. Two milliliters of blood was drawn at 18.5, 19.5, 20.5, and 22.5 h after DES treatment and held briefly on ice before plasma isolation at 1,470 *g* for 20 min at 4°C. Plasma TAG was determined enzymatically, and samples with the highest TAG content were shipped on ice from California to Maryland within 24 h for parallel isolation of VLDL and determination of VLDL particle diameter distributions using instruments in both the Maryland and California laboratories.

The timing of the VLDLy enrichment protocol was the same in subsequent studies (**Fig. 1**). Food was removed on the evening before intubation (6 PM) to minimize intestinal content, and unfed birds were injected with DES 18 h later (12 noon). Birds were intubated with emulsions at 5 h after DES injection (5 PM) and returned to feed for 6 h (lights on). Food was again removed to allow for the metabolism of LPL-susceptible VLDL; birds were anesthetized at 22 h after DES injection (10 AM, 17 h after emulsion intubation) and exsanguinated by cardiac puncture. Plasma was separated, held, and transported on ice during the 24 h before lipoprotein separation.

In study 2, two cockerels were intubated with 5 ml containing 1 g of [1-^{13}C]palmitate-enriched emulsions each, and two cockerels were intubated with equivalent amounts of native lipid emulsions. All birds were intubated with 25 ml of 0.04 M sodium cholate in water soon after emulsion intubation. A third pair of birds was intubated with 25 ml of 0.04 M sodium cholate and served as vehicle-intubated controls. During the 6 h interval in which food was provided, cockerels intubated with either [1-^{13}C]palmitate-enriched or native lipid emulsions were fed the basal low-fat diet, whereas the cholate-intubated controls were fed the basal diet supplemented with 6% corn oil to equalize total fat consumption.

In study 3, cockerels weighing 0.4–0.6 kg were used. Two cockerels were intubated with 5 ml of emulsion containing 1 g of tri-[1-^{13}C]oleoylglycerol and 0.5 g of [1-^{13}C]palmitate, and two cockerels were intubated with emulsion containing equivalent amounts of native lipids. All cockerels were provided access to the basal low-fat diet until 11 h after DES injection.

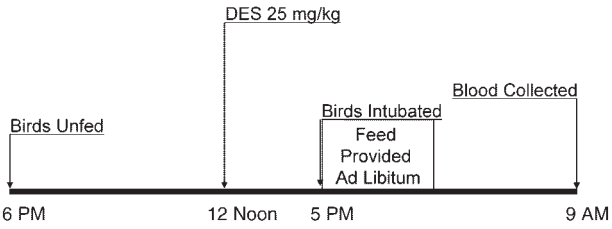

Fig. 1. Timeline for yolk-deposited very low density lipoprotein (VLDLy) induction and isotope enrichment protocol. DES, diethylstilbestrol.

Separation of VLDLy

Approximately 10 ml of plasma was recovered from each bird. An aliquot of plasma from each bird was retained, and the bulk was sent on ice via express delivery to Maryland for NMR analysis. Within 36 h of blood draw, VLDLy were isolated from plasma by density ultracentrifugation, and the isolated VLDLy fraction was held at 4°C before analysis. Within 24 h of isolation, 0.5 ml of neat VLDLy was placed directly into 5 mm NMR tubes, and ^{13}C NMR spectra were obtained. Density solutions used to isolate VLDLy for NMR analysis were prepared in 99.9% deuterium oxide to provide a lock signal.

Biochemical analysis

After the addition of heptadecanoic acid as an internal standard, total lipid was extracted from 50 μl aliquots of VLDLy using a modified Folch extraction (31). One-half of the lipid extract was methylated by the addition of 2 ml of acetyl chloride-methanol (1:15) and held at 60°C for 2 h. Tridecanoic fatty acid methyl ester was added as a second internal standard after methylation. The resulting fatty acid methyl esters were separated by gas chromatography on an HP 5890 series II gas chromatograph equipped with a flame ionization detector and a DB-23 capillary column (J&W Scientific, Folsom, CA), peak identity was assigned relative to retention times of authentic standards (Nuchek 68A), and individual fatty acid amounts were calculated by area relative to internal standards. To determine the fatty acid composition of individual lipid classes, 10 μl aliquots of VLDLy lipid extract were plated onto thin-layer chromatography plates (Whatman), overlaid with 20 μg of cholesterol nonadecanoate (19:0) as an internal standard, and separated with hexane-ethyl ether-formic acid (80:20:2) (32). CE, TAG, free fatty acids, and PL bands were scraped from thin-layer chromatography plates and extracted from silica with benzene before methylation, and gas chromatography analysis was performed as described above. Total cholesterol was measured by enzymatic assay. Total protein was measured using a modified micro-Lowry assay with BSA as the standard (Sigma kit P-5656).

Particle diameter analysis

Aliquots of neat VLDLy were transferred to a glass cuvette containing 1 ml of water to yield an intensity output of >200 kHz on the PSS Nicomp model 370 submicron particle analyzer (Santa Barbara, CA) or diluted with saline and placed directly into the analytical cell of a Microtrac 9200 (Microtrac, Clearwater, FL) (17, 33). Data were collected in five cycles of 5 min each. Lipoprotein particle diameter distributions were determined both before and immediately after NMR analysis. Diameter distribution is presented as mean particle diameter ± SD on a number-weight basis.

Analysis of ^{13}C isotopic enrichment by GC-MS

Fatty acid methyl esters prepared as described above were separated and identified using a Hewlett-Packard model 6890 gas chromatograph equipped with an HP-5 capillary column and a Hewlett-Packard 5973 mass selective mass spectrometer (Wilmington, DE). Ion fragments were identified using the National Institute of Standards and Technology Mass Library Spectra Database (18).

^{13}C NMR spectroscopy

^{13}C NMR spectra were acquired at 75.6 MHz using a QE 300 NMR spectrometer (Fremont, CA). A 5 mm $^{1}H/^{13}C$ probe was used with parameters set to either maximize the signal-to-noise ratio (sweep width, 20,000 Hz; block size, 16,000 points; excitation pulse, 60°; recycle time, 2.5 s; with broadband heteronuclear decoupling) or adjusted to determine T_1 relaxation times and nuclear Overhauser enhancement (NOE) values for measurable carbonyl resonances. T_1 relaxation times of carbonyl resonances were determined according to the methods of Opella, Nelson, and Jardetzky (34). The number of acquisitions ranged from 2,000 to 36,000 depending on the sample and specific experiment. Samples were spun at a rate of 17–19 Hz. Spectra were obtained at 25 and 37°C after ^{1}H NMR analysis of a sucrose standard and the VLDLy sample for comparison of magnetic homogeneity. Data were analyzed using MacFID software by Teqmag (Houston, TX) and treated with baseline correction and exponential multiplication of 0.5–3.0 Hz before Fourier transformation. Chemical shift values (δ) were referenced to the terminal methyl carbon of lipid acyl chains at 14.10 ppm (13). Peak assignments for surface-located lipids were made based on published values for TAG in PC vesicles (13–16), and assignments for core TAG were based on published values of TAG in lipoprotein particles (19). Line width at half-height, area, and signal intensity values were measured digitally using MacFID software. To compare the relative intensity of resonances within a single spectrum, areas were normalized to the *sn*-1,3 carbonyl resonance of TAG in the core set to 100.

Calculation of ^{13}C enrichment by NMR

The ratio of the integrals of carbonyl signals to terminal methyl signals from the spectra of VLDLy obtained from cockerels intubated with [1-^{13}C]palmitate and tri-[1-^{13}C]oleoylglycerol or comparable non-^{13}C-enriched lipids was used to calculate the amount of ^{13}C enrichment over natural abundance. The ratio was multiplied by the natural abundance of ^{13}C (1.11%) to yield total ^{13}C enrichment (35). When comparing intensity of resonances between different spectra, variation in signal intensity resulting from differences in the concentration of lipid or the number of acquisitions was eliminated by normalizing peak areas to the terminal methyl carbon in each spectra. The ratio of terminal methyl carbons to carbonyl carbons of either TAG or PL was constant regardless of total lipid concentration.

Estimation of surface lipid content

The percentage of TAG in the surface (% $TAG_{SURFACE}$) versus the core of VLDLy was calculated from the ratio of areas of ^{13}C carbonyl resonances of TAG in the core and surface phases corrected for NOE, as described by Hamilton and Small (13) according to equation 1.

$$\%\ TAG_{SURFACE} = \frac{(\text{Area } TAG_{SURFACE})}{(\text{Area } TAG_{SURFACE} + \text{Area } TAG_{CORE})} \times 100 \qquad \textit{(Eq. 1)}$$

The mass of TAG in the surface phase was calculated based on the % $TAG_{SURFACE}$ and the chemical analysis of TAG in VLDLy after NMR (TAG_{VLDLy}) according to equation 2.

$$\text{mg } TAG_{SURFACE} = \%\ TAG_{SURFACE} \times \text{mg } TAG_{VLDLy} \qquad \textit{(Eq. 2)}$$

It was assumed that the total mass of PL and 85% of UC determined via chemical analysis of VLDLy after NMR (mg PL_{VLDLy} and UC_{VLDLy}) was located at the surface (8, 36). The total lipid mass of the surface was calculated from equation 3.

$$\text{mg Lipid}_{SURFACE} = \text{mg } TAG_{SURFACE} + \text{mg } PL_{VLDLy} + 0.85\ (\text{mg } UC_{VLDLy}) \qquad \textit{(Eq. 3)}$$

The weight percentage of TAG in VLDLy ($SurfaceTAG_{WT\%}$, $SurfaceTAG_{MOL\%}$) was calculated according to equation 4.

$$SurfaceTAG_{WT\%} = \text{mg } TAG_{SURFACE}/\text{mg Lipid}_{SURFACE} \qquad \textit{(Eq. 4)}$$

Lipid weights were converted to moles using the average molecular weight calculated for TAG from the fatty acid profile (**Table 2**). An average molecular weight of 770 was used for PL. Values were then used to calculate the mol% surface content of each lipid. The limitations and assumptions used to estimate surface lipid content were as follows: *1*) integration accuracy of the small surface TAG peaks relative to core TAG peaks; *2*) number of samples analyzed; and *3*) the assumption that TAG carbonyls in surface and core phases experience similar mechanisms and degrees of relaxation during acquisition. An alternative approach to estimate the surface lipid content would calculate the ratio of signal intensities of surface TAG carbonyl peaks to PL carbonyl peaks. Although this approach was considered, it was not used because the estimates generated would carry additional uncertainty introduced by the accuracy of ^{13}C lipid class enrichment determinations (17). Based on the limitations and assumptions used, the experimental error for $TAG_{SURFACE}$ was estimated to be ±15% of the calculated value.

RESULTS

Production of VLDLy

VLDLy accumulation in plasma was monitored by increases in plasma TAG concentration coincident with reductions in VLDL particle diameter. The VLDL diameter decreased from 70 ± 5 nm before DES injection to 58 ± 4, 50 ± 6, and 29 ± 1 nm at 4, 7, and 20 h after dosing, respectively. Experiments conducted 18–22.5 h after DES injection confirmed that infused free fatty acid, using pentadecanoic acid as a marker, was incorporated into VLDLy lipid pools (data not shown).

Composition of VLDLy

Lipid and protein compositions of VLDLy recovered from [1-^{13}C]palmitate- and tri-[1-^{13}C]oleoylglycerol-intubated cockerels did not differ from those of cockerels intubated with emulsions prepared with native lipid and were typical of normal laying hen VLDLy composition. The fractional composition of the analyzed VLDLy particles was 22.4% PL, 58.1% TAG, 2.8% CE, 4.6% UC, and 12.1% protein by weight. There were no significant differences in total protein content, lipid-to-protein ratio, or particle diameter distribution of VLDLy isolated from ^{13}C-intubated and native lipid groups. The mean particle diameter of VLDLy used in all studies was 23.6 ± 2.2 nm (n = 6). The results of GC-MS analysis of the fatty acid profile and corresponding ^{13}C isotopic enrichment of TAG, PL, and CE of VLDLy varied between the tri-[1-^{13}C]oleoylglycerol- and [1-^{13}C]palmitate-intubated birds, as shown in Ta-

TABLE 2. Fatty acid profiles and ^{13}C isotopic enrichment of TAG, CE, and PL extracted from ^{13}C-enriched VLDLy

	Tri-[1-^{13}C]oleoylglycerol and [1-^{13}C]palmitate[a]						[1-^{13}C]palmitate[b]					
Fatty Acid	TAG		CE		PL		TAG		CE		PL	
	% FA	*% ^{13}C*	*% FA*	*% ^{13}C*	*% FA*	*% ^{13}C*	*% FA*	*% ^{13}C*	*% FA*	*% ^{13}C*	*% FA*	*% ^{13}C*
15:0	1.2 ± 0.2				0.4 ± 0.02		0.4 ± 0.01				0.11 ± 0.1	
16:0	25.0 ± 1.7	18.0	22.8 ± 0.4	9.8	32.8 ± 5.6	13.8	24.5 ± 1.9	5.0	40.9 ± 2.6	2.2	29.4 ± 2.2	16.6
16:1	2.6 ± 0.5	9.3	1.4 ± 0.4	nm[c]	0.4 ± 0.02	nm	3.2 ± 0.2	⩽1.0			0.8 ± 0.2	14.4
18:0	5.1 ± 1.0	2.8	4.7 ± 0.1	5.83	17.4 ± 1.3	6.8	6.9 ± 0.6	⩽1.0	18.0 ± 1.8	3.8	23.3 ± 2.1	1.6
18:1n9	53.0 ± 1.0	52.0	27.7 ± 3.1	32.9	19.0 ± 2.6	41.9	33.0 ± 2.5	4.2	30.8 ± 2.1	2.7	16.1 ± 1.8	1.9
18:2n6	11.0 ± 0.5	⩽1.0	33.0 ± 0.3	⩽1.0	16.2 ± 1.1	⩽1.0	17.6 ± 1.3	2.1	10.3 ± 1.6	⩽1.0	15.4 ± 1.4	⩽1.0
18:3n3	0.4 ± 0.1	nm	0.6 ± 0.2	nm	0.1 ± 0.1	nm	0.2 ± 0.04	nm				
20:4n6	0.4 ± 0.04	nm	3.5 ± 0.2	nm	8.6 ± 0.5	nm	0.4 ± 0.01	nm			8.9 ± 1.5	nm
Other	1.1 ± 0.4		5.7 ± 1.7		5.6 ± 0.1							
Average molecular weight	852.4		661.8				859.2		657.9			
Average ^{13}C[d]		32.4		13.3		12.1		3.1		2.5		5.7

CE, cholesteryl ester; PL, phospholipid; TAG, triacylglycerol; VLDLy, yolk-targeted very low density lipoprotein. Values are percentages of total fatty acids and are averages of duplicate analyses, with two birds per treatment. Total lipid was separated by TLC after internal standard addition into TAG and PL fractions. Isolated lipid classes were scraped from the plates, methylated, and quantified using added internal standard by GC with a flame-ionization detector. ^{13}C isotopic enrichment was determined from mass spectral data.

[a] From VLDLy of tri-[1-^{13}C]oleoylglycerol- and [1-^{13}C]palmitate-infused birds.

[b] From VLDLy of [1-^{13}C]palmitate-infused birds.

[c] nm, not measured.

[d] Average molecular ^{13}C enrichment.

ble 2. In cockerels intubated with emulsions containing tri-[1-^{13}C]oleoylglycerol, the ^{13}C isotopic enrichment of oleic acid was 52% in TAG, 42% in PL, and 32% in CE, indicating a high degree of preformed oleic acid incorporation into each of these lipid classes.

^{13}C enrichment of intact VLDLy

The ^{13}C NMR spectra of intact native VLDLy from tri-[1-^{13}C]oleoylglycerol- and [1-^{13}C]palmitate- as well as native lipid-intubated roosters are shown in **Fig. 2**. It was apparent from the intensity of TAG and PL carbonyls in the VLDLy of ^{13}C-intubated birds compared with the spectra of birds intubated with native lipids (Fig. 2) that the [1-^{13}C]palmitate and tri-[1-^{13}C]oleoylglycerol were incorporated directly into the TAG and PL pools. ^{13}C enrichment of TAG carbonyls from tri-[1-^{13}C]oleoylglycerol- and [1-^{13}C]palmitate-intubated samples was estimated to be 28% and 6%, respectively, over natural abundance from ratios of TAG carbonyl to terminal methyl resonances in these spectra (**Table 3**). The calculated isotopic enrichment of TAG carbonyls via ^{13}C NMR was in reasonable agreement with the enrichment values calculated from mass spectrometry of fatty acid methyl esters of TAG (Table 2).

Surface-located TAG was present in VLDLy, as shown in the ^{13}C NMR spectrum and enlarged carbonyl region of VLDLy (**Fig. 3A**, **B**). In the order of decreasing chemical shift values (δ), the carbonyl resonances in the spectrum of VLDLy (Fig. 3A, **Table 4**) were as follows: PL carbonyls, *sn*-1,3 carbonyls of TAG in the surface ($TAG_{SURFACE1,3}$), *sn*-2 carbonyls of TAG in the surface ($TAG_{SURFACE2}$), *sn*-1,3 carbonyls of TAG in the core ($TAG_{CORE1,3}$), and *sn*-2 carbonyls of TAG in the core (TAG_{CORE2}). Figure 3B indicates the location of spinning side bands when present. In the order of decreasing chemical shift values, the carbonyl resonances in the spectrum of VLDLy with spinning side bands (Fig. 3B) were as follows: PL carbonyls, $TAG_{SURFACE1,3}$, two spinning side band artifacts located at +35 and +17 Hz from $TAG_{CORE\ 1,3}$, $TAG_{CORE1,3}$, and two spinning side band artifacts located at −18 and −32 Hz from TAG_{CORE2}. Note that the spectrum in Fig. 3B was obtained under suboptimal shimming conditions. The carbonyl resonance for $TAG_{SURFACE2}$ is obscured by the spinning side band at +35 Hz in Fig. 3B; however, it can be reliably assigned as $TAG_{SURFACE2}$ in Fig. 3A because there are no apparent spinning side bands in this spectrum. The $TAG_{SURFACE2}$ resonance is also distinguished from a spinning side band in Fig. 3A by its frequency difference from the major peak, +29 Hz compared with +35 Hz.

Changes in chemical shift values, and the difference in chemical shift values between TAG located in the surface and core of VLDLy, provide separate strong evidence of the positioning of TAG in the surface of VLDLy (Table 4). The ^{13}C chemical shifts of PL and acylglycerol carbonyls are exquisitely sensitive to hydration, with a documented downfield shift (i.e., increase in ppm) with either an increase in hydration or solvent polarity (37, 38). The differences in chemical shift values (Δδ) between $TAG_{SURFACE1,3}$ and $TAG_{CORE1,3}$ is 0.8 ppm in VLDLy, much less than the 1.3 ppm typical of TAG in PL vesicles or the 1.2 ppm typical of emulsions containing long-chain TAG (13, 17). This indicates different contributions from the physical environment on the $TAG_{SURFACE1,3}$ carbonyl resonances between VLDLy and vesicles or emulsions. Changes in the physical environment that could affect chemical shifts include differences in hydration, the lateral packing density of lipids, or the radius of curvature of VLDLy lipids compared with vesicles or emulsions. Changes in the radius of curvature of the inner versus the outer leaflet of PL vesicles can result in a chemical shift change of ~0.2 ppm for PC (17). Because the change in chemical shift for TAG was >0.2 ppm, particle diameter may contribute to the changes noted here but would not completely explain the observation. It is more likely that hydration and packing density had the greater effect. Specifically, the smaller

downfield chemical shift indicates that surface-located TAG in VLDLy may be less hydrated than surface TAG in vesicles or emulsions, and/or that the TAG has a different molecular orientation and degree of mobility arising from the lateral packing density of surface lipids in VLDLy.

DISCUSSION

The mean surface lipid composition of VLDLy was calculated as 5.1 ± 0.6 mol% TAG, 26.3 ± 0.3 mol% UC, and 68.6 ± 0.5 mol% PL. These values translate to 6.7 ± 0.8 wt% TAG, 13.9 ± 0.1 wt% UC, and 79.3 ± 0.7 wt% PL. The amount of $TAG_{SURFACE}$ was significantly ($P < 0.02$) greater than the 3.6 ± 0.6 wt% determined using physically separated phases of emulsions prepared from human VLDL (8). Each VLDLy particle contains one integral apoB-100 molecule in combination with other apolipoproteins, primarily the estrogen-induced apolipoprotein $apoVLDL_{II}$ (39). Like apoB-100, $apoVLDL_{II}$ is a nonexchangeable (i.e., integral) apolipoprotein (39). ApoB-100 has a pentapartite structure that surrounds the lipoprotein particle and is partially embedded in the surface shell, contributing to the surface area and particle integrity (6, 40, 41). Sequenced portions of avian apoB-100 are similar to those of human apoB-100 (42). The structural contributions of integral apolipoproteins such as apoB-100 and $apoVLDL_{II}$ could be expected to affect the fundamental solubility and hydration of $TAG_{SURFACE}$ in TAG-rich lipoproteins.

It is intriguing that VLDLy, a TAG-rich lipoprotein with well-documented resistance to LPL hydrolysis, would have significantly more surface-located TAG than human VLDL

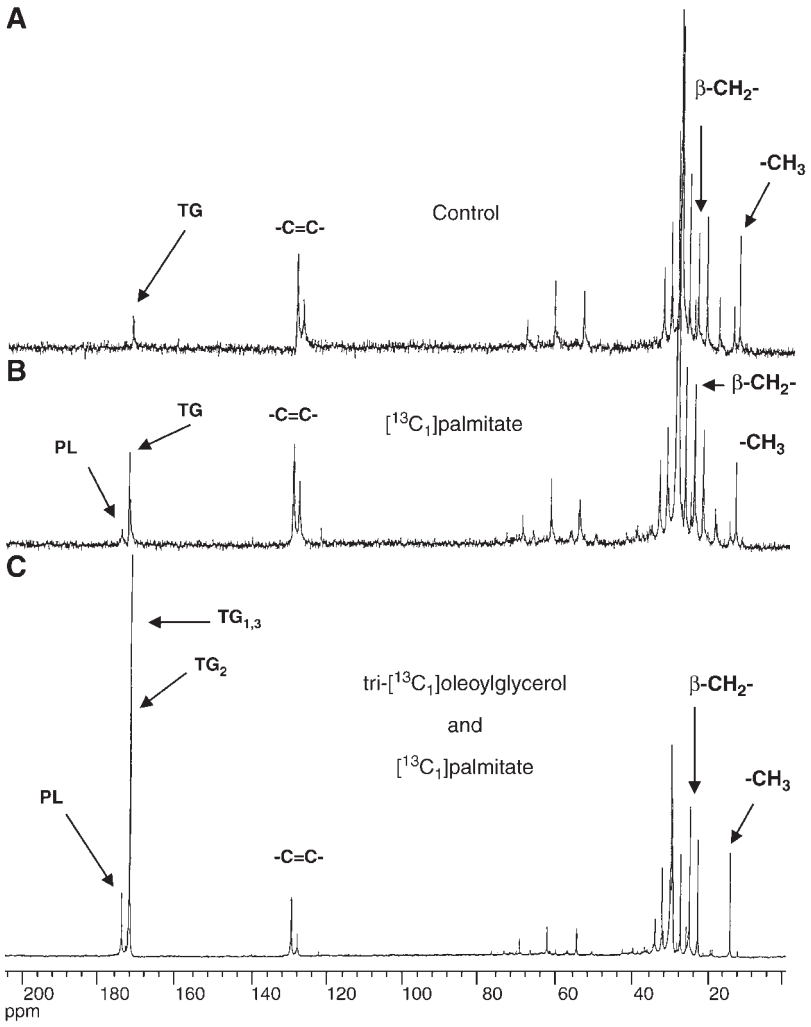

Fig. 2. ^{13}C NMR spectra of native VLDLy processed with baseline correction, 3.0 Hz line broadening, and Fourier transformation. VLDLy was from birds infused with native lipid, 36,000 scans (A), [1-^{13}C]palmitate, 35,000 scans (B), and tri-[1-^{13}C]oleoylglycerol and [1-^{13}C]palmitate, 36,000 scans (C). Peaks are referenced to the terminal methyl carbon at 14.10 ppm and identified as the phospholipid (PL) carbonyls, *sn*-1,3 carbonyls of triacylglycerol (TAG) in the core ($TG_{1,3}$), *sn*-2 carbonyls of TAG in the core (TG_2), olefinic carbons (-C=C-), β-methylene carbons (β-CH_2-), and the terminal methyl carbons (-CH_3). Particle diameter distributions (mean particle diameter ± SD on a number-weighted basis) of VLDLy from each sample were 26.2 ± 4 nm (A), 25.4 ± 5 nm (B), and 23.1 ± 4 nm (C).

TABLE 3. Relative areas of selected resonances in ^{13}C NMR spectra of native and ^{13}C isotopically enriched VLDLy

Resonance	Chemical Shift	Area			
		Palmitate		Trioleoylglycerol and Palmitate	
		[^{12}C][a]	[1-^{13}C][b]	[^{12}C]	[1-^{13}C]
	δ *ppm*				
PL carbonyl	173.6	<0.2[a]	1.8[c]	0.4	16.5[c]
TAG carbonyl$_{SURFACE}$	172.6	—	—	—	1.7[c]
TAG carbonyl$_{CORE}$	171.8	2.8	14.1[d]	2.1	52.3[c]
-CH=CH-	130.0	26.4	28.2	14.8	18.9
Glycerol -CH_2-	62.0	8.9	10.9	3.6	4.8
-CH_2-CH_2-CH_2-	29.9	190.8	195.5	91.9	126.1
CH=CH-CH_2-CH=CH	25.9	7.7	8.8	4.6	5.4
-CH_2-CH_2-COOH	25.1	16.8	27.5[d]	8.5	29.2[c]
Terminal methyl	14.1	10.0	10.0	10.0	10.0

Values are from ^{13}C NMR spectra of neat VLDLy and are averages of duplicate samples from each of two birds per treatment group. Spectra were processed with 3.0 Hz exponential line broadening, integrated digitally, and referenced to the terminal methyl carbon.

[a] Insufficient signal intensity to integrate. Values are from NMR spectra of VLDLy from birds intubated with matched native lipids.

[b] Values are from NMR spectra of VLDLy from birds intubated with ^{13}C-enriched lipids.

[c] Resonances are significantly different from those of matched controls at $P < 0.05$ by Student's *t*-test.

[d] Resonances are significantly different from those of matched controls at $P < 0.01$ by Student's *t*-test.

(8). It was proposed that apoVLDL$_{II}$ inhibits LPL by interfering with the ability of either the enzyme or its cofactor apoC-II to bind to VLDLy (27, 28). The physical evidence of a lower $\Delta\delta$ value between TAG$_{SURFACE1,3}$ and TAG$_{CORE1,3}$ in VLDLy compared with PC vesicles or emulsions suggests that apoVLDL$_{II}$ serves as a physical barrier between VLDLy TAG$_{SURFACE1,3}$ and water. Reduced TAG$_{SURFACE}$ hydration would reduce VLDLy susceptibility to LPL by preventing or interfering with the interaction between essential reactants for LPL-catalyzed hydrolysis. Alternatively, TAG$_{SURFACE}$ may adopt a different molecular conformation in the surface of VLDLy, making the TAG carbonyls less available to hydration, or hydration may influence protein conformation and thus the ability of apoC-II or LPL to interact with the surface. ApoVLDL$_{II}$ rather than apoB-100 is expected to mediate this effect, as avian VLDLs lacking apoVLDL$_{II}$ are readily hydrolyzed (27). Either possibility provides potential mechanisms to explain VLDLy's known resistance to LPL hydrolysis.

Our data show marked differences in $\Delta\delta$ between *sn*-1,3 and *sn*-2 TAG carbonyls in the surface of VLDLy (0.3 ppm) and the TAG present in the surface of PL vesicles (0.7 ppm) prepared from acyl-heterogenous TAG isolated from birds used in the present study (18). Vesicles provide a useful model system in which to test the effects of various components on lipid partitioning within a highly hydrated environment. For comparison, the $\Delta\delta$ of *sn*-1,3 and *sn*-2 TAG carbonyls in the core of VLDLy or the excess oil phase of vesicles is a similar ~0.3 ppm (Table 4) (8, 15, 18). Thus, the $\Delta\delta$ of TAG carbonyls in the surface of VLDLy indicates that *sn*-1,3 carbonyls remain somewhat more exposed to the polar environment than *sn*-2 carbonyls, but not nearly to the extent as TAG present in the surface of PL vesicles. These differences indicate that the molecular conformation of the TAG$_{SURFACE}$ differs in VLDLy and PL vesicles.

The observation of two sets of narrow peaks for TAG in VLDLy indicates that the rate of exchange of TAG between the surface and core in VLDLy is slow on the NMR time scale. The lower limit for the residence time in either the surface or the core can be calculated using the difference in chemical shift between the two resonances measured in hertz ($\Delta\nu$) to determine the lifetime (τ) of a nucleus in one of two possible chemically shifted resonances (43). For TAG between the surface and core of VLDLy, $\Delta\nu \sim 59$ Hz and the residence time of TAG at either the surface or the core is $\geq$7.5 ms. This is similar to values observed for the residence time of cholesterol in either the surface or core of HDL, $\geq$10 ms (21).

The surface solubility of TAG in PC vesicles has been used to predict the amount of surface-located TAG in lipoprotein particles. In vesicles, the amount of surface-located TAG is dependent on TAG fatty acyl chain length, the total lipid composition of the particle, and the temperature of sample preparation and analysis (2, 13–17). For example, a UC content of 20 mol% or greater, as was observed in native VLDLy particles, reduces surface TAG solubility within PC vesicles (15). Miller and Small (36) reported that surface-located TAG in physically separated emulsions prepared from triolein, cholesteryl oleate, and egg yolk lecithin decreased from 4.5 to 1.8 wt% when UC content of the emulsion was increased from 2 wt% (14 mol%) to 5.1 wt% (33 mol%). These observations suggest that in the absence of apolipoproteins, increases in UC content effectively reduce surface-located TAG content.

PL vesicles devoid of UC and fabricated to contain the acyl-heterogenous TAG extracted from the livers of birds used in the present study had a maximum surface-located TAG solubility of 3.4 $\pm$ 0.4 mol% (18), making it unlikely that the greater TAG$_{SURFACE}$ content of intact VLDLy resulted from differences in TAG fatty acyl chain length or composition. Nor are the differences attributable to temperature, because ^{13}C NMR spectra were acquired at 37°C, within 2 K of published measurements for TAG$_{SURFACE}$ in model systems (13–15). The mean particle diameter of VLDLy was in the range of PC vesicle diameters (20–30 nm) used in previous measurements of TAG$_{SURFACE}$ (13–15). The major differences between previous measurements of TAG$_{SURFACE}$ and those reported here are the intact structure of the native lipoprotein particles and specifically the presence of integral apolipoproteins. Based on results from vesicles and emulsions, it could be predicted that the presence of UC would reduce the amount of TAG$_{SURFACE}$ in VLDLy compared with UC-free PC vesicles. However, this was not the case, and the greater than expected amount of TAG$_{SURFACE}$ in intact VLDLy appears to be the result of structural contributions from apolipoprotein moieties of the intact VLDLy particle.

In summary, substantially more surface-located TAG was present in intact native apoB-100-containing lipoproteins than would be predicted from PC vesicle or emulsion model systems containing similar amounts of UC. More-

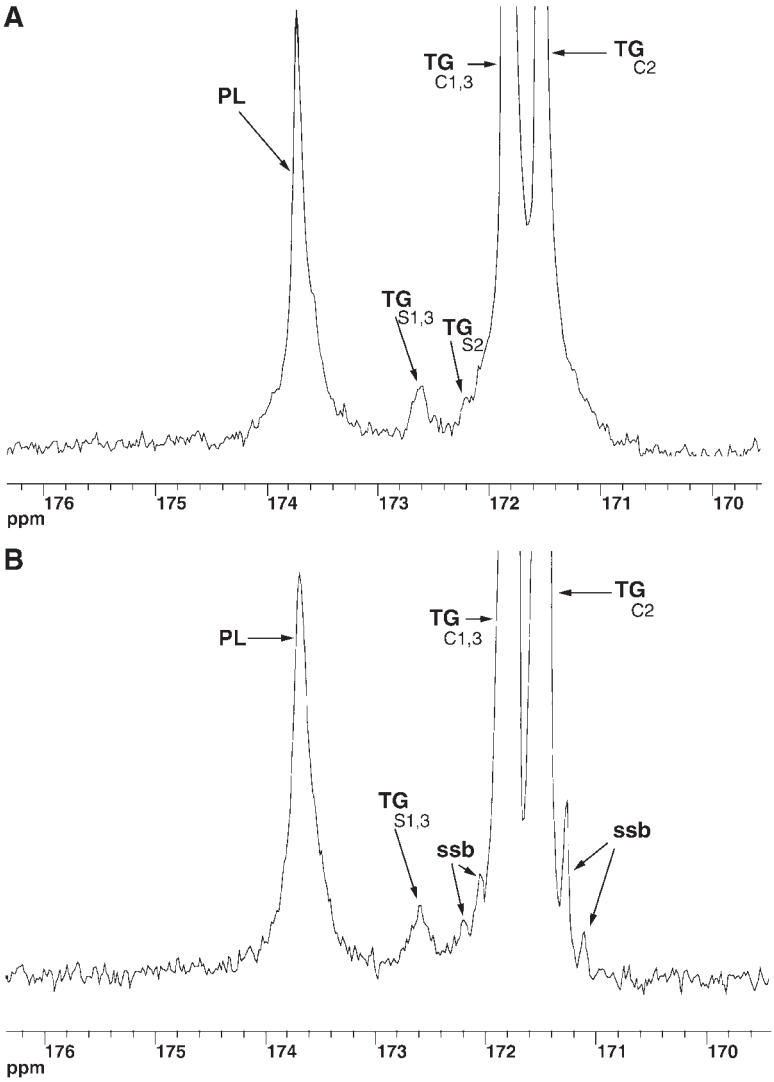

Fig. 3. Enlarged carbonyl region of ^{13}C NMR spectrum of VLDLy recovered from cockerels intubated with 1.0 g of tri-[1-^{13}C]oleoylglycerol and 0.5 g of [1-^{13}C] palmitate. A: The spectrum represents 2,048 acquisitions processed with baseline correction, exponential multiplication of 1.5 Hz, and Fourier transformation. Peaks are referenced to the terminal methyl carbon at 14.10 ppm and identified as the PL carbonyls, *sn*-1,3 carbonyls of TAG in the surface ($TG_{S1,3}$), *sn*-2 carbonyls of TAG in the surface (TG_{S2}), *sn*-1,3 carbonyls of TAG in the core ($TG_{C1,3}$), and *sn*-2 carbonyls of TAG in the core (TG_{C2}). The TG_{S2} peak is +29 Hz from the major peak $TG_{C1,3}$. B: The spectrum represents 20,000 acquisitions processed with baseline correction exponential multiplication of 1.0 Hz and Fourier transformation. Peaks are identified as PL carbonyls, *sn*-1,3 carbonyls of TAG in the surface ($TG_{S1,3}$), spinning side bands (ssb), *sn*-1,3 carbonyls of TAG in the core ($TG_{C1,3}$), *sn*-2 carbonyls of TAG in the core (TG_{C2}), and spinning side bands (ssb). From downfield to upfield, spinning side bands are +35 and +17 Hz from $TAG_{C1,3}$, and −18 and −32 Hz from TAG_{C2}.

over, $TAG_{SURFACE}$ was less hydrated and/or in a different molecular conformation in native VLDLy lipoprotein particles compared with apolipoprotein-free lipid vesicles. These factors indicate that apoB-100 and $apoVLDL_{II}$ provide structural support that accommodates greater amounts of TAG in the surface of colloidal particles. Additionally, $apoVLDL_{II}$ may serve as a barrier to hydration and so mediate VLDLy's well-known resistance to LPL-mediated lipid hydrolysis. It remains to be determined whether other apoB-100 or apoB-48 particles show class-specific differences in surface lipid content that result in differences in substrate properties. The combination of specific ^{13}C isotopic enrichment and ^{13}C NMR provides a powerful strategy for distinguishing factors that influence the composition of lipids in the surface of intact native lipoproteins.

TABLE 4. T_1 relaxation times, line widths, and NOE values for lipid carbon resonances in VLDLy

Resonance	Chemical Shift	T_1	Line Width[a]	NOE
	δ ppm	*s*	*Hz*	
PL	173.70	2.2 ± 0.2	11.3 ± 2.2	1.2
$TAG_{SURFACE1,3}$	172.61	1.9 ± 0.8	10.2 ± 1.2[b]	1.2
$TAG_{SURFACE2}$	172.28	nm[c]	6.1 ± 1.2[b]	nm
$TAG_{CORE1,3}$	171.82	2.2 ± 0.3	2.8 ± 1.0	1.3
TAG_{CORE2}	171.53	1.6 ± 0.4	2.4 ± 0.5	1.3
Terminal methyl	14.10		2.2 ± 1.1	

NOE, nuclear Overhauser enhancement. Chemical shift values are referenced to the terminal methyl carbon. T_1 relaxation time and NOE were calculated from a single VLDLy sample.

[a] Line width is the average of VLDLy from two birds.

[b] Values measured manually.

[c] nm, not measurable.

E.B-R. gratefully acknowledges financial support from the American Heart Association, Maryland Affiliate (MGBG0795), the International Life Sciences Institute Future Leader Award Program 1997–1999, and the Maryland Agriculture Experiment Station. R.L.W. gratefully acknowledges financial support from the National Institutes of Health (5 RO1 HL-60844-02) and the Texas Agricultural Experiment Station (Project 8738). The authors thank Dr. Yiu-fai Lam, Gabriel Corneliscu, Claudia Corneliscu, and Dr. Walter Schmidt for technical assistance with NMR; Mona Khan, Li Chen, and Shilpa Padmanaban for assistance with biochemical analysis; Dr. Scott Rankin and Rong Li for mass spectrometry; and Vanessa Meunoit, Gabe Smith, and Gina Brower for assistance with bird intubations.

REFERENCES

1. Small, D. M., S. Bennett-Clark, A. Tercyak, J. Steiner, D. Gantz, and A. Derksen. 1991. The lipid surface of triglyceride-rich particles can modulate (apo)protein binding and tissue uptake. *In* Hypercholesterolemia, Hypocholesterolemia, Hypertriglyceridemia. C. L. Malmendier, P. Alaupovic, and H. B. Brewer, Jr., editors. Plenum Press, New York. 281–298.
2. Deckelbaum, R. J., J. A. Hamilton, A. Moser, G. Bengtsson-Olivecrona, E. Butbul, Y. A. Carpentier, A. Gutman, and T. Olivecrona. 1990. Medium-chain versus long-chain triacylglycerol emulsion hydrolysis by lipoprotein lipase and hepatic lipase: implications for the mechanisms of lipase action. *Biochemistry.* **29:** 1136–1142.
3. Borgstrom, B. 1980. Importance of phospholipids, pancreatic phospholipase A_2, and fatty acids for the digestion of dietary fat: in vitro experiments with the porcine enzymes. *Gastroenterology.* **78:** 954–962.
4. Sammet, D., and A. R. Tall. 1985. Mechanisms of enhancement of cholesteryl ester transfer protein activity by lipolysis. *J. Biol. Chem.* **260:** 6687–6697.
5. Mims, M. P., and J. D. Morrisett. 1988. Lipolysis of phospholipids in model cholesteryl ester rich lipoproteins and related systems: effect of core and surface lipid phase state. *Biochemistry.* **27:** 5290–5295.
6. Schumaker, V. N., M. L. Phillips, and J. E. Chatterton. 1994. Apolipoprotein B and low-density lipoprotein structure: implications for biosynthesis of triglyceride-rich lipoproteins. *Adv. Protein Chem.* **45:** 205–248.
7. Segrest, J. P., M. K. Jones, and N. Dashti. 1999. N-terminal domain of apolipoprotein B has structural homology to lipovitellin and microsomal triglyceride transfer protein: a "lipid pocket" model for self-assembly of apoB-containing lipoprotein particles. *J. Lipid Res.* **40:** 1401–1416.
8. Miller, K. W., and D. M. Small. 1983. Surface-to-core and interparticle equilibrium distributions of triglyceride-rich lipoprotein lipids. *J. Biol. Chem.* **258:** 13772–13784.
9. Miller, K. W., and D. M. Small. 1987. Structure of triglyceride-rich lipoproteins: an analysis of core and surface. *In* Plasma Lipoproteins. A. M. Gotto, editor. Elsevier, Amsterdam, The Netherlands. 1–72.
10. Manchekar, M., P. E. Richardson, T. M. Forte, G. Datta, J. P. Segrest, and N. Dashti. 2005. Apolipoprotein B-containing lipoprotein particle assembly. *J. Biol. Chem.* **279:** 39757–39766.
11. Shelness, G. S., L. Hou, A. S. Ledford, J. S. Parks, and R. B. Weinberg. 2003. Identification of the lipoprotein initiating domain of apolipoprotein B. *J. Biol. Chem.* **278:** 44702–44707.
12. Wang, J., H. Liu, B. D. Sykes, and R. O. Ryan. 1995. Identification and localization of two distinct microenvironments for the diacylglycerol component of lipophorin particles by ^{13}C NMR. *Biochemistry.* **34:** 6755–6761.
13. Hamilton, J. A., and D. M. Small. 1981. Solubilization and localization of triolein in phosphatidylcholine bilayers: a ^{13}C NMR study. *Proc. Natl. Acad. Sci. USA.* **78:** 6878–6882.
14. Hamilton, J. A., K. W. Miller, and D. M. Small. 1983. Solubilization of triolein and cholesteryl oleate in egg phosphatidylcholine vesicles. *J. Biol. Chem.* **258:** 12821–12826.
15. Spooner, P. J., and D. M. Small. 1987. Effect of free cholesterol on incorporation of triolein in phospholipid bilayers. *Biochemistry.* **26:** 5820–5825.
16. Hamilton, J. A., J. M. Vural, Y. A. Carpentier, and R. J. Deckelbaum. 1996. Incorporation of medium chain triacylglycerols into phospholipid bilayers: effect of long chain triacylglycerols, cholesterol, and cholesteryl esters. *J. Lipid Res.* **37:** 773–782.
17. Boyle-Roden, E., and M. A. Khan. 2001. Quantitative analysis of surface-located triacylglycerol in intact emulsion particles. *J. Agric. Food Chem.* **49:** 2014–2021.
18. Li, R., W. Schmidt, S. Rankin, R. L. Walzem, and E. Boyle-Roden. 2003. Solubilizaton of acyl heterogeneous triacylglycerol in phosphatidylcholine vesicles. *J. Agric. Food Chem.* **51:** 477–482.
19. Hamilton, J. A., and J. D. Morrisett. 1986. Nuclear magnetic resonance studies of lipoproteins. *Methods Enzymol.* **128:** 472–515.
20. Sears, B., R. J. Deckelbaum, M. J. Janiak, G. Shipley, and D. M. Small. 1976. Temperature-dependent ^{13}C nuclear magnetic resonance studies of human serum low density lipoproteins. *Biochemistry.* **15:** 4151–4157.
21. Lund-Katz, S., and M. C. Phillips. 1984. Packing of cholesterol molecules in human high-density lipoproteins. *Biochemistry.* **23:** 1130–1138.
22. Lund-Katz, S., and M. C. Phillips. 1986. Packing of cholesterol molecules in human high-density lipoprotein. *Biochemistry.* **25:** 1562–1568.
23. Luskey, K. L., M. S. Brown, and J. L. Goldstein. 1974. Stimulation of the synthesis of very low density lipoproteins in rooster liver by estradiol. *J. Biol. Chem.* **249:** 5939–5947.
24. Walzem, R. L. 1996. Lipoproteins and the laying hen: form follows function. *Poult. Avian Biol. Rev.* **7:** 31–64.
25. Walzem, R. L., R. J. Hansen, D. L. Williams, and R. L. Hamilton. 1999. Estrogen induction of VLDLy assembly in egg-laying hens. *J. Nutr.* **129 (Suppl.):** 467–472.
26. Williams, D. L. 1979. Apolipoproteins of avian very low density lipoprotein: demonstration of a single high molecular weight apolipoprotein. *Biochemistry.* **18:** 1056–1063.
27. Griffin, H., G. Grant, and M. Perry. 1982. Hydrolysis of plasma triacylglycerol-rich lipoproteins from immature and laying hens (*Gallus domesticus*) by lipoprotein lipase in vitro. *Biochem. J.* **206:** 647–654.
28. Schneider, W. J., R. Carroll, D. L. Severson, and J. Nimpf. 1990. Apolipoprotein VLDL-II inhibits lipolysis of triglyceride-rich lipoproteins in the laying hen. *J. Lipid Res.* **31:** 507–513.
29. Park, J. R., and B. H. Cho. 1990. Effects of estrogen on very-low-density lipoprotein triacylglycerol metabolism in chicks. *Biochim. Biophys. Acta.* **1045:** 180–186.
30. Walzem, R. L., S. Watkins, E. N. Frankel, R. J. Hansen, and J. B. German. 1995. Older plasma lipoproteins are more susceptible to oxidation: a linking mechanism for the lipid and oxidation theories of atherosclerotic cardiovascular disease. *Proc. Natl. Acad. Sci. USA.* **92:** 7460–7464.
31. Folch, J., M. Lees, and G. H. Sloane-Stanley. 1957. A simple method for the isolation and purification of total lipides from animal tissues. *J. Biol. Chem.* **226:** 497–509.
32. Christie, W. W. 1973. Lipid Analysis: Isolation, Separation, Identification and Structural Analysis of Lipids. Pergamon Press, Oxford, UK.
33. Walzem, R. L., P. A. Davis, and R. J. Hansen. 1994. Overfeeding increases very low density lipoprotein diameter and causes the appearance of a unique lipoprotein particle in association with failed yolk deposition. *J. Lipid Res.* **35:** 1354–1366.
34. Opella, S. J., D. J. Nelson, and O. Jardetzky. 1976. Nuclear magnetic resonance description of molecular motion and phase separations of cholesterol in lecithin dispersions. *J. Chem. Phys.* **64:** 2533–2535.
35. Harris, R. K. 1986. Nuclear Magnetic Resonance Spectroscopy. A Physiochemical View. Longman Scientific and Technical, Essex, UK.
36. Miller, K. W., and D. M. Small. 1983. Triolein-cholesteryl oleate-cholesterol-lecithin emulsions: structural models of triglyceride-rich lipoproteins. *Biochemistry.* **22:** 443–451.
37. Soulages, J. L., M. Rivera, F. A. Walker, and M. A. Wells. 1994. Hydration and localization of diacylglycerol in the insect lipoprotein lipophorin. A ^{13}C-NMR study. *Biochemistry.* **33:** 3245–3251.
38. Okamura, E., T. Kimura, M. Nakahara, M. Tanaka, T. Handa, and H. Saito. 2001. ^{13}C NMR method for the determination of peptide and protein binding sites in lipid bilayers and emulsions. *J. Phys. Chem. B.* **105:** 12616–12621.
39. Miller, K. W., and M. D. Lane. 1984. Estradiol-induced alteration of very-low-density lipoprotein assembly. Possible competition among apolipoproteins for incorporation into nascent very low density lipoproteins. *J. Biol. Chem.* **259:** 15277–15286.
40. Segrest, J. P., M. K. Jones, V. K. Mishra, G. M. Anantharamaiah, and D. W. Garber. 1994. ApoB-100 has a pentapartite structure composed of three amphipathic alpha-helical domains alternating with two amphipathic beta-strand domains. Detection by the computer program LOCATE. *Arterioscler. Thromb.* **14:** 1674–1685.
41. Chatterton, J. E., M. L. Phillips, L. K. Curtiss, R. Milne, J. C. Fruchart, and V. E. Schumaker. 1995. Immunoelectron microscopy of low density lipoproteins yields a ribbon and bow model for conformation of apolipoprotein B on the lipoprotein surface. *J. Lipid Res.* **36:** 2027–2037.
42. Segrest, J. P., M. K. Jones, V. K. Mishra, V. Pierotti, S. G. Young, J. Borén, T. L. Innerarity, and N. Dashti. 1998. Apolipoprotein B-100: conservation of lipid-associating amphipathic secondary structural motifs in nine species of vertebrates. *J. Lipid Res.* **39:** 85–102.
43. Abraham, R. J., and P. Loftus. 1979. Proton and Carbon-13 NMR Spectroscopy. Heyden, London. 165–168.